Mécanique & Industries 9, 335–346 (2008)
www.mecanique-industries.org
© AFM, EDP Sciences 2008
DOI: 10.1051/meca:2008038

Mécanique & Industries

Improvement of the railway vehicle performance in circulation in curve

Habib Bettaieb[a]

Laboratoire de Génie Mécanique ENIM, Université de Monastir, Av. Ibn El Jazzar, 5019 Monastir, Tunisie
École Préparatoire aux Académies Militaires, 4052 Sousse, Tunisie

Received 27 September 2007, Accepted 7 August 2008

Abstract – This article paper the influence of rails inclination on the behaviour of a railway vehicle in circulation on a curve and on alignment. A comparative study is performed the behaviour of a vehicle which circulates on rails without inclination and another circulating on inclined on rails. This study shows the interest on the inclined rails. The effects of the transverse and longitudinal stiffness of the primary suspension, the angle of inclination rail and the equivalent conicity of the wheels are considered to evaluate the vehicle's behaviour in curve and transverse stability. The simulation of the vehicle moving in curve with inclined rails shows that the transverse displacement of this vehicle decreases if the inclination of the rails increases. Moreover, the stability of a wheelset which circulates on inclined rails is comparable to the stability of a wheelset which circulates on the rail without inclination, and then the stability of the vehicle is preserved.

Key words: Simulation / movement in curve / rail inclination / transverse stability / critical speed

Résumé – Amélioration des performances des véhicules ferroviaires en circulation en courbe. Cet article simule l'influence de l'inclinaison des rails sur le comportement d'un véhicule ferroviaire en circulation sur une voie en courbe et en alignement. Une étude comparative est réalisée sur le comportement d'un véhicule qui circule sur des rails sans inclinaison et un autre circulant sur des rails inclinés ; cette étude a montré l'intérêt de l'inclinaison des rails. Les effets de la rigidité des ressorts transversal et longitudinal de la suspension primaire, de l'angle d'inclinaison du rail et de la conicité équivalente des roues ont été considérés pour évaluer le comportement du véhicule en courbe et la stabilité transversale. Les résultats de la simulation numérique fournissent les caractéristiques mécaniques à donner à un véhicule pour avoir un déplacement transversal des essieux minimum et une vitesse critique maximale. La simulation du comportement du véhicule en circulation en courbe sur des rails inclinés montre que le déplacement transversal de ce véhicule diminue si l'inclinaison des rails augmente. Par ailleurs, la stabilité d'un essieu qui circule sur des rails inclinés, est comparable à la stabilité d'un essieu qui circule sur le rail sans inclinaison, alors la stabilité du véhicule est préservée.

Mots clés : Simulation / circulation en courbe / rail incliné / stabilité transversale/ vitesse critique

1 Introduction

It is well known that the railway vehicle should be able to operate at a high speed while achieving acceptable performance in a curve in terms of reduced wear of wheels and rail. In the design of the railway vehicle there is a conflict between dynamic stability at a high speed and the ability of the vehicle to steer around curves [1,2]. The majority of the existing vehicles are optimized in stability of alignment, but not in circulation in curve. Such a matter induces problems of maintenance of both wheel and rail. Among these problems, one can notice the wear of the wheel as well as that of the rail cost much money to the railway companies and creates the danger of derailment. Over the years, wheel and rail wear has been extensively studied. Some of these studies were tested in laboratory, the challenge consists of how to implement laboratory test results on a real wheel and rail system. A number of investigations have worked on improving the rail vehicle design between the stability and the curving performance.

Boocok [3] considered the steady-state motion of bogie and two wheelset vehicles. Special attention was given

[a] Corresponding author: habib.bettaieb@enim.rnu.tn

Nomenclature

C_{11}, C_{22}, C_{23} and C_{33}	Creep coefficients of Kalker
e_j	Distances between the centre of inertia of the wheelset and the wheel and rail points of contact
e_0	Half distance between the contact points in the central position
I_x	Wheelset moment of inertia about axis x
I_y	Wheelset moment of inertia about axis y
I_z	Wheelset moment of inertia about axis z
K_x	Longitudinal stiffness of primary suspension
K_y	Lateral stiffness of primary suspension
Ky	Lateral stiffness of secondary suspension
M_{kij}	Spin creep moment
m	Wheelset mass
M	Bogie mass
$\overline{M}$	Body mass
r_0	Rolling circle radius for a central position
R_c	Curve radius
r_j	Rolling circle radius of the wheel and rail points of contact
R'	Transverse radius of rail profile
R	Transverse radius of wheel profile
T_{kij}	Transverse creep forces
V	Velocity vehicle along track
X_{kij}	Longitudinal creep forces
z	Height of wheelset centre
β	Rail inclination
γ_e	Wheel equivalent conicity
Φ_{kij}	Spin at the contact point j
w_{Nkij}	Angular velocity about normal in contact point j
ν_{kij}	Creepages at the contact point j
One maintains the values	below constant, except in case where there is a variation of the constant (K_x, R_c, γ_e, β)
$e_0 = 0.75$ m	Half distance between the contact points in the central position
$\overline{Kx} = 1.73 \times 10^5$ N.m^{-1}	Longitudinal stiffness of secondary suspension
$K_x = 5 \times 10^6$ N.m^{-1}	Longitudinal stiffness of primary suspension
$K_y = 5 \times 10^6$ N.m^{-1}	Lateral stiffness of primary suspension
$m = 1500$ kg	Wheelset mass
$M = 3020$ kg	Bogie mass
$\overline{M} = 43\,200$ kg	Car body mass
$R_c = 2000$ m	Curve radius
$R = f(\beta; \gamma_0; \gamma_e; e_0; r_0)$	Transverse radius of wheel profile
$r_0 = 0.45$ m	Rolling circle radius for a central position
$R' = 0.3$ m	Transverse radius of rail profile
$R_1 = \infty$	Longitudinal radius of rail profile
$\beta = 0$	Rail inclination
$\gamma_e = 0.2$	Wheel equivalent conicity
$\gamma_e = 0.025$	Wheel equivalent conicity (new wheelset)

to the effect of primary and secondary suspension parameters and the results were evaluated with experiments.

Rao et al. [4] considered the steady state motion of conventional bogie and two wheelset's vehicle, the effects of unsymmetrical suspensions were also included. Many designs are considered to provide good dynamic performance and the ability of the vehicle to steer round a curve.

Arus et al. [5] have shown the importance of curving behavior and the geometric problem in the presence of single and double contact between rail and wheel. Single point contact which takes place in a large domain of velocities for large curves disappears for tight curves and small cant angles.

Cheli et al. [6] have developed a numerical model for the simulation of dynamic behavior of a tilted railway body vehicle for increasing train speed in curves (20 to 25% more than in conventional vehicle).

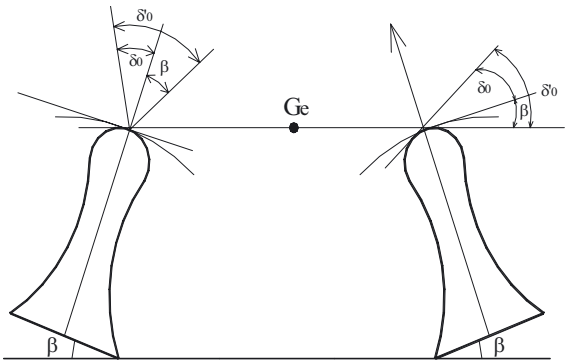

Fig. 1. Inclined rail.

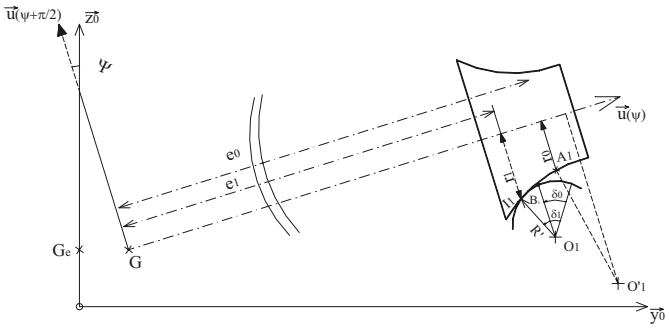

Fig. 2. Wheelset parameters.

To solve wheel and rail wear problem, Sato [7] suggests conceiving a new shape of the wheel profile and rail, taking into account worn wheels and rails. This change of profile has attenuated the wear of the wheels and rail only in large radius curves.

Leary et al. [8] developed a second suggested solution, based on the design of an interchangeable standard profile for the railway of North America which aims at reducing the rail-wheel wear, hence reducing the risk of derailment and stabilizing the performances of the vehicle in alignment. Two approaches are used to build the profile. One method employs a form of profile based on the models of the damaged wheels (100 worn wheels). The second method results from a profile of wheels in conformity with the shape of rail ensuring only one contact point (the damaged rail sections are used to determine the typical profiles of a new rail). Thus, the suggested solution cannot be generalized to all the circuits, and requires working on worn elements to obtain the desired form of the profile.

Smith [9] suggested improving the geometry of the interface between rail and wheel. The author proposes the variation of the equivalent conicity of the wheel. This variation must ensure conformity of the profiles of the wheel and the rail, which reduces wear. To obtain a good curving performance and to avoid having two contact points, it is possible to use a profile design by the combination of two or several radii of curves.

The solutions suggested by the authors listed above do not bring total satisfaction to the problems of wheel and rail wear nor to the speed limit of the vehicles in circulation in a curve. The aim of the present work is to use a rail inclination. The study of variation of rail inclination on the motion of the vehicle is considered. This will allow us to master the transverse displacement of the wheelset, to avoid flange contact in a curve, which causes high wear on the wheel and the rail while preserving a good stability in alignment. This will reduce the cost of maintenance and will improve the comfort of the passengers (Fig. 1).

2 The model

We have to define with precision the parameters used in the mechanical model. The steps followed in this process begin with the geometrical study of the wheel and rail contact. This study will allow us to provide the necessary relations in order to determine the distances e_j, r_j between the centre of inertia of the wheelset and the wheel and rail points of contact as a function of the position parameters of the wheelset and rail inclination as shown in Figure 2. Non-linear geometrical wheel-rail points of contact characteristics are considered. The contact angle and other contact parameters can be calculated from the wheelset transverse displacement y and yaw angle α. The application of the Kalker's theory [10] determines the actions of contact between the rail and the wheel. The application of the Lagrange's formalism to the relative motion will provide the dynamic behavior of the vehicle. The dynamic model is built on the basis of a set of differential equations. This model can be reduced to a set of algebraic equations by using the equilibrium position, where accelerations and velocities tend to zero (Kineto-static). The numerical resolution of the system of equations is obtained using a MATLAB software. Both results for transverse displacements and critical speed of wheelset are functions of the construction parameters of the vehicle, the inclination rail and the curve characteristics. A railway vehicle is taken as a multiple rigid body system composed of wheelset, bogie frames and car body as seen in Figure 3.

These rigid bodies are connected to each other by elements of suspension, primary and secondary suspensions. The dampers are put in parallel with the springs. It should be mentioned that for the investigations of the curving behaviour, the values of the body's centrifugal forces due to transverse curvature of the truck central line are introduced. It is assumed that the transverse and the vertical vibrations of the system are uncoupled, thus, only the transverse vibrations of the system are taken into consideration for this analysis. The system has 17 degrees of freedom. The wheelset is given with an index $i = 1$ (leading wheelset) and $i = 2$ (trailing wheelset), a contact point on the wheel tread is indicated by the index $j = 1$ (left wheel) and $j = 2$ (right wheel), the bogie frame is given with an index $k = 1$ (the first), and $k = 2$ (the second). For all solids the movements considered are the lateral displacement, the yaw (rotation around axis Z) and the rolling (rotation around axis X).These movements are noted as follows:

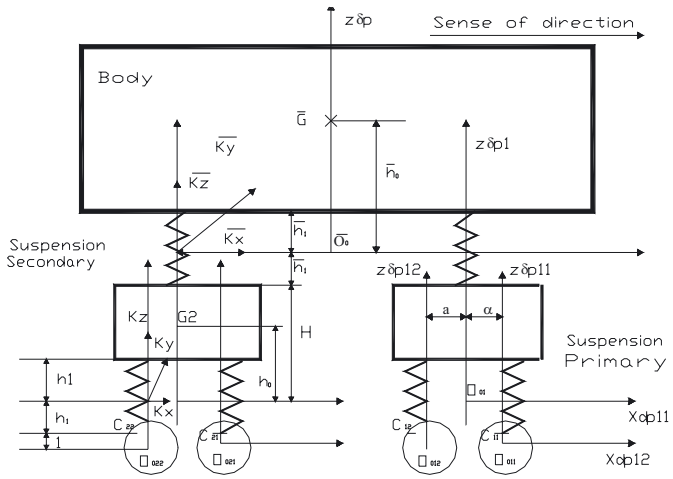

Fig. 3. Vehicle model.

- the car body (C): $\bar{y}\bar{\alpha}, \bar{\theta}$
- the bogie frames (C_k): $Y_k\alpha_k$, θ $k = 1, 2$ (Y_1, Y_2, α_1, α_2, θ_1, θ_2)
- the wheelsets (S_{ki}): $y_{ki}; \alpha_{ki}; \psi_{ki}$ $k = 1, 2$ $i = 1, 2$ ((y_{11}, y_{12}, y_{21}, y_{22}, α_{11}, α_{12}, α_{21}, α_{22}, $\psi_{11=}f(y_{11})$, $\psi_{12} = f(y_{12})$, $\psi_{21} = f(y_{21})$, $\psi_{22} = f(y_{22})$).

2.1 Geometrical contact

The geometrical contact study allows us to determine the main geometrical elements which are in function of the geometry of rail and wheel for a vehicle moving on inclined rails. Thus, it must provide us with formulas to evaluate the distances between the centre of inertia and the points of contact as function of the position parameters of the wheelset and rail inclination. If one considers the real form of the rail and the wheel, the motion of the wheelset on the rail has a corresponding double point of contact. On the one hand, a point of contact is on the rail, on the other hand, another point is on the wheel (see Appendix A). Near the points of contact, one can consider that the real profiles of rail and wheels are circular. One denotes R and R' the corresponding radii of curvature of the wheel and the rail profile respectively, whereas δ_0 is the contact angle for for a central position. One also denotes:
the β: rail inclination;
$\delta'_0 = \beta + \delta_0$;
r_0: the rolling circle radius for a central position;
e_0: the half distance between the contact points in the central position;
ψ : the rolling angle of the wheelset.

During the wheelset movement, these quantities become respectively, r_j, e_j, ψ_{ki} where $j = 1$ for the left wheel in the direction of advance and $j = 2$ for the right wheel. The wheel and rail geometrical contact parameters are considered as non-linear functions of the wheelset transverse displacement y_{ki}, yaw angle α_{ki}, wheel rolling radius r_0, transverse radius of wheel profile R', rail inclination angle β, wheelset roll angle ψ and transverse radius of rail profile R. According to the geometry contact study, one defines the useful formulas to build the dynamic model. The rail profile is constant, whereas one describes the wheel profile by means of the functions $R = f(\gamma_e)$ and $r_1 = f(y)$.

$$e_j = e_0 + (-1)^j y \frac{R\cos\delta'_0}{R - R'}\left(\frac{e_0 + R'\sin\delta'_0}{e_0\cos\delta'_0 - r_0\sin\delta'_0}\right)$$
$$= e_0 + (-1)^j .y.\gamma_e.\mathrm{cotg}\,\delta'_0 \quad (1)$$

$$r_j = r_0 + (-1)^{j+1} y \frac{R\sin\delta'_0}{R - R'}\left(\frac{e_0 + R'\sin\delta'_0}{e_0\cos\delta'_0 - r_0\sin\delta'_0}\right)$$
$$= r_0 + (-1)^{j+1}\, y.\gamma_e \quad (2)$$

$$\psi_{ki} = y_{ki}\frac{\sin\delta'_0}{e_0\cos\delta'_0 - r_0\sin\delta'_0} = y_{ki}.\Gamma$$

$$\varepsilon_1 = -\alpha\mathrm{tg}(\gamma'_0) \quad (3)$$

$$\gamma_e = \frac{R\sin\delta'_0}{R - R'}\left(\frac{e_0 + R'\sin\delta'_0}{e_0\cos\delta'_0 - r_0\sin\delta'_0}\right) \quad \text{and}$$

$$\Gamma = \frac{\sin\delta'_0}{e_0\cos\delta'_0 - r_0\sin\delta'_0} \quad (4)$$

$$\delta'_0 = \delta_0 + \beta \quad (5)$$

2.2 Wheel and rail interactive forces

The longitudinal, transverse creep forces and spin creep moments are calculated using Kalker's linear creep theory only for small creepage (case of circulation in alignment and large radius curve).

$$X_{kij} = -C_{11}.\boldsymbol{\nu}_{kij}.\boldsymbol{x}_0$$
$$T_{kij} = -C_{22}.\boldsymbol{\nu}_{kij}.\boldsymbol{u}(\gamma_j) - C_{23}.\Phi_{kij}$$
$$M_{kij} = C_{23}.\boldsymbol{\nu}_{kij}.\boldsymbol{u}(\gamma_j) - C_{33}.\Phi_{kij} \quad (6)$$

where $\boldsymbol{x}_0$, $\boldsymbol{u}(\gamma_j)$ defines the tangent plan to the point of contact I_{kij}. C_{11}, C_{22}, C_{23} and C_{33} are the creep Kalker coefficients which depend on elasticity modulus, the Poisson's ratio, and the ratio between the semi–axes ellipse contact. The creepages and spin at the contact point are defined as:

$$\Phi_{kij} = \frac{w_{N_{kij}}}{V} \quad \text{and} \quad w_{N_{kij}} = \boldsymbol{w}^g_{S_{ki}}.\boldsymbol{u}\left(\gamma_j + \frac{\pi}{2}\right) \quad (7)$$

$$\boldsymbol{\nu}_{kij} = \frac{\boldsymbol{g}(S_{ki}/\mathrm{rail}, I_j, t)}{|V_g(I_j)|} \quad (8)$$

These quantities depend on the characteristics of the contact point, the rolling radius and the contact angle. The

dissipated power by the contact forces can be written as follows:

$$P = \sum_{k=1}^{2}\sum_{i=1}^{2}\sum_{j=1}^{2}\left(X_{kij}\boldsymbol{V}(\boldsymbol{I}_{kij}).x_0 + \boldsymbol{T}_{kij}\boldsymbol{V}(\boldsymbol{I}_{kij}).\boldsymbol{u}(\gamma_j) + M_{kij}\boldsymbol{w}_S\boldsymbol{u}\left(\gamma_j + \frac{\pi}{2}\right)\right) \quad (9)$$

Having completely defined the coordinate system, one can calculate the kinetic energy T, and the potential energy V of the vehicle. The set of differential equations can then be derived by applying Lagrange's equations.

2.3 Motion on a curve

The dynamic model of the complete vehicle includes 17 degrees of freedom. Some assumptions were adopted for the dynamic study of the vehicle in circulation in a curve:

- the vehicle moves with a constant speed;
- the system is at equilibrium and there is a small force on the wheel;
- the curve radius R_C is constant and sufficiently large.

Then one can neglect, in a first approximation, the damping forces and the inertia forces compared to the elastic forces

2.3.1 Variable of relative positions

It is assumed that the vehicle is rigid with nominal geometry describing perfect track design. The track centre line, which is an element of nominal geometry, always stays in horizontal plan. In a curve of constant radius, a free motion wheelset in a railway takes a stable position, which corresponds to a motion of rolling without slip. This position has a transverse displacement y_0. This position will be taken as the origin of the transverse displacements. One writes:

$$y_0 = \frac{e_0.r_0}{\gamma_e.R_c} \quad y_k = y_k^* + \frac{y_{k1}^* + y_{k2}^*}{2} + y_0 \quad (10)$$

$$y_{ki} = y_{ki}^* + y_0 \quad \overline{Y} = \frac{\overline{Y_1} + \overline{Y_2}}{2}$$

$$\alpha_k = \alpha_k^* + \frac{y_{k1}^* - y_{k2}^*}{2a} \quad \overline{\alpha} = \frac{\overline{Y_1} - \overline{Y_2}}{2\overline{A}} \quad (11)$$

$\overline{Y_1}$ and $\overline{Y_2}$ are the transverse displacements of two points of the car body and coincide with the geometric axis of two bogie frames. The rolls of the different solids are neglected in the motion on a curve. Taking into account all the calculations [1], one finds the following expressions of the transverse displacement of the car body and the two bogie frames (12) and two uncoupled systems describe the motions of the two bogies and the four wheelsets (13).

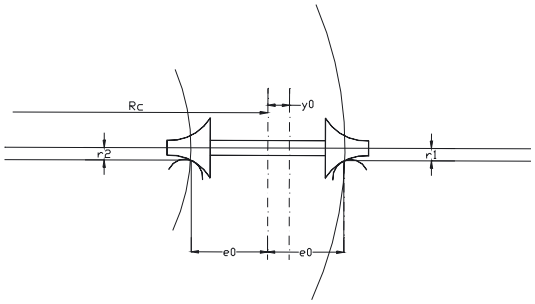

Fig. 4. Wheelset position in a curve.

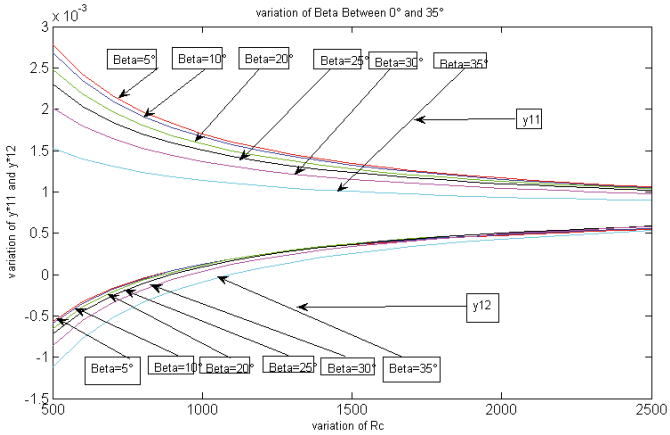

Fig. 5. Wheelset transverse displacement as function of R_c.

Each bogie and two wheelsets have 5 degrees of freedom, such as α yaw of bogie; y_{11}, y_{12} transverse displacement of the wheelsets; α_{11}, α_{12} yaw of the wheelsets [1]. with these conditions the dynamic study of a complete vehicle can be replaced by a bogie and two wheelsets taking account of the total weight of the vehicle (Fig 4).

$$\overline{Y_1} = \overline{Y_2} = \frac{\overline{M}}{4\overline{K}y}\left(\frac{V^2}{R_c}\right) \quad \text{and}$$

$$Y_1^* = Y_2^* = \frac{M + (\overline{M}/2)}{4Ky}\left(\frac{V^2}{R_c}\right) \quad (12)$$

$$[K(X)]\{X\} = \{B\} \quad (13)$$

The steady-state curve problem is solved using nonlinear Equation (13) where K is the suspension stiffness matrix and B is the external force acting on the vehicle and where $\{X\} = \{\alpha, y_{ij}, \alpha_{ij}\}^T$ $i = 1$ and $j = 1{,}2$. The analytical technique used is the iteration method of the set of equation of motion. To start the iterative procedure, it is necessary to have an approximate solution.

2.3.2 Simulation results

Figure 5 shows the transverse displacement $(y_{11}^*; y_{12}^*)$ as function of R_c, for various inclination angles β (0°, 10°, 20°, 25°, 30° and 35°). For the large curves (R_c >1000 m)

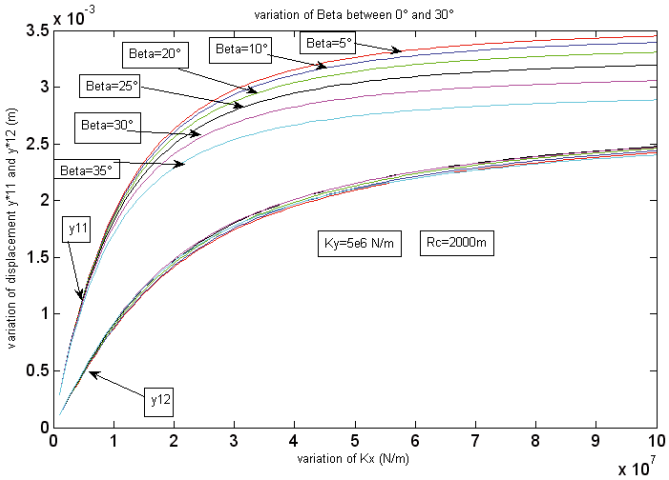

Fig. 6. Wheelset transverse displacement as function of the longitudinal stiffness of primary suspension.

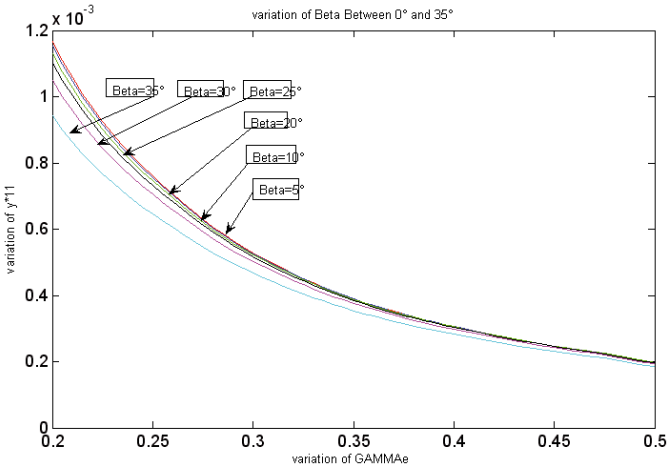

Fig. 7. Wheelset transverse displacement as function of the equivalent conicity γ_e.

the transverse displacement decreases, and it increases for tight curves and small rail inclination β. When the radius of the curve increases, the transverse displacement of the vehicle becomes small and constant. y_{11}^* is always positive y_{12}^* negative; the leading wheelset moves towards the outside of the curve; the trailing wheelset takes a centred position in the railway (confirmed by the experimental results) [11].

Figure 6 shows the variations of the transverse displacement y_{11}^* as function of the longitudinal stiffness of primary suspension K_x, for various rail inclination angles β (0°, 10°, 20°, 25°, 30° and 35°), and for a transverse constant stiffness of primary suspension $K_y = 5 \times 10^6$ N.m^{-1}, $R_c = 500$ m. For a constant radius curve R_c, the transverse displacement increases for high value of longitudinal stiffness of primary suspension K_x [1,11]. On the other hand, the transverse displacement decreases for high value of rail inclination. It shows that stiffness of primary suspension K_x and inclination rail β have a great influence on the transverse displacement of wheelset. A soft stiffness of primary suspension on leading wheelset reduces the transverse displacement in the traffic on a curve. In this case, the wheel–rail wear decreases. Railway companies confirm these results by experiment.

Figure 7 shows the transverse displacement (y_{11}^*) as a function of the wheel conicity γ_e. For a constant radius curve $R_c = 500$ m, and different incline angles β, the transverse displacement of the leading wheelset decreases when γ_e increases. For small wheel conicity, there is an evident flange contact, which causes more interaction efforts and yields a high wear of the wheels and rail. For a constant radius of a curve R_c, the transverse displacement of the vehicle decreases when β increases. When the equivalent conicity of the wheel increases, the transverse displacement of the vehicle becomes small and constant.

Figure 8 shows the yaw angle of the leading wheelset as a function of the longitudinal primary stiffness K_x. For a constant radius of the curve and different angles of the rail (0°, 10°, 20°, 25°, 30° and 35°), the yaw angle

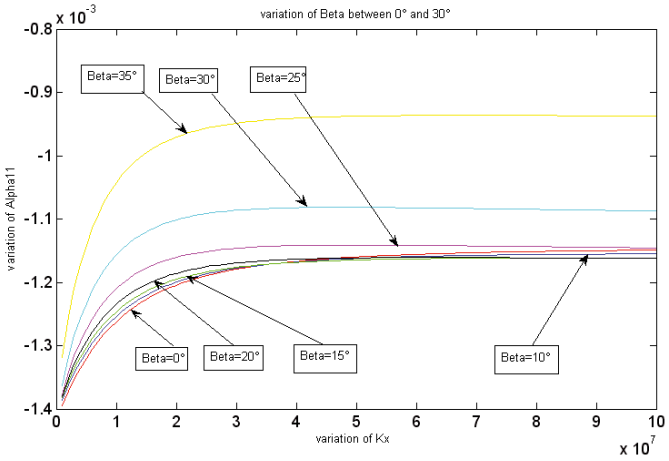

Fig. 8. Yaw angle α_{11} as function of the longitudinal stiffness of primary suspension.

increases with the incline angle β. Starting from the value of longitudinal rigidity $K_x = 4 \times 10^7$ N.m^{-1} of the primary suspension, the wheelset takes a position of stable hunting in the curve.

Figure 9 shows respectively the yaw angle of the leading and the trailing wheelset, as functions of curve radius R_c. For various angles β (0°, 10°, 20°, 25°, 30° and 35°), the yaw angle decreases when the curve radius increases. For a constant radius of the curve and different angles β of the rail inclination, the yaw angle increases with the angle β.

3 Dynamic stability

The wheelset transverse motion is an important problem for railway vehicle. One was interested in studying the wheelset dynamic effect circulating on rail inclination. This study allowed us to determine the critical speed of free wheelset. In order to investigate the wheelset transverse dynamic, one allows three degrees of freedom to the

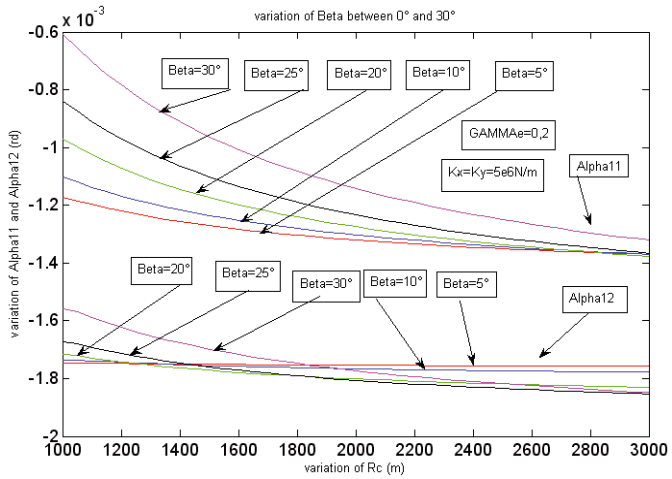

Fig. 9. First and second wheelset yaw angle α_{11}, α_{12} as function of R_c (curve radius).

wheelset model: yaw α (about axis z), the transverse displacement y and rolling ψ (about axis x), where:

$$\psi_{=}\Gamma.y \quad \text{with} \quad \Gamma = \frac{\sin\delta_0}{e_0.\cos\delta_0 - r_0\sin\delta_0} \tag{14}$$

The equation of motion of the free wheelset can be written as:

$$[M]\{x^{\bullet\bullet}\} + [C]\{x^{\bullet}\} + [K]\{x\} = \{0\} \tag{15}$$

where $\{x\} = \{y, \alpha, \psi\}^T$ and $[M]$, $[C]$ and $[K]$ are mass, damping, and stiffness matrices respectively. They are functions of the structural parameters (masses, dampers, etc.). The stiffness and damping matrices are also function of the velocity, due to the linearized contribution of the rail-wheel contact forces, inclination angle β, wheel equivalent conicity γ_e, load W, various geometric variables (1), (2),..., (5) and creep coefficients C_{11}, C_{22}, C_{23} and C_{33}. The load per wheelset W, inclination rail β and equivalent conicity γ_e are chosen here as design variables, the value of all other parameters are fixed. The stability analysis can be performed using the Equations (15) of the free motion of the wheelset. Equation (15) cannot be transformed into an uncoupled set of differential equations by means of conventional methods of modal analysis, i.e., using only real modes. A solution can be found using the complex modal transformation

$$D = \begin{bmatrix} [0] & [I]_{2x2} \\ -[M]^{-1}[K] & -[M]^{-1}[C] \end{bmatrix} \tag{16}$$

$$M = \begin{bmatrix} a_v & \\ 0 & a_{vp} \end{bmatrix} \quad C = \begin{bmatrix} b_v & b_{v1} \\ b_{vp1} & b_{vp} \end{bmatrix} \quad K = \begin{bmatrix} c_v & c_{v1} \\ c_{vp1} & c_{vp} \end{bmatrix} \tag{17}$$

$$a_v = m.d^2 + I_x \qquad a_{vp} = I_z \tag{18}$$

$$b_v = \frac{2C_{22}.\chi^2}{V(\cos\delta)^2} \qquad b_{v1} = -\frac{V.T.I_y}{r_0} + \frac{2.C_{23}.\chi}{V} \tag{19}$$

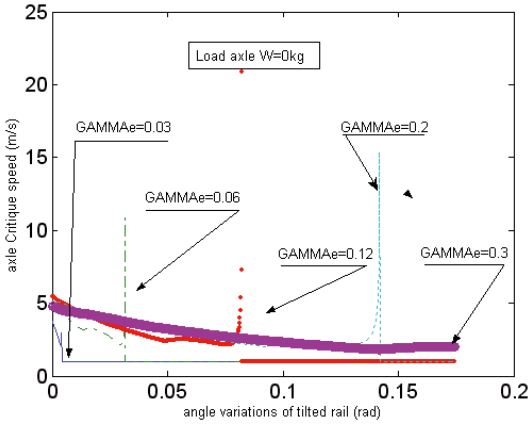

Fig. 10. Wheelset critical speed as function of rail inclination angle ($W = 0$ kg).

$$b_{vp} = \frac{2C_{11}.e_0^2.}{V} + \frac{2C_{33}.\chi(\cos\delta)^2}{V} \tag{20}$$

$$b_{vp1} = \frac{V.T.I_y}{r_0} - \frac{2.C_{23}.\chi}{V} \tag{21}$$

$$c_{v1} = \frac{-2C_{22}.\chi}{(\cos\delta)^2} \qquad c_v = w.g.\varphi - \frac{2.C_{23}.\chi.\gamma_e}{R.r_0.\sin\delta} \tag{22}$$

$$c_{vp} = 2.C_{23} - w.g.\varepsilon_0 tg\delta$$

$$c_{vp1}\frac{2C_{11}.\gamma_e.e_0.}{r_0} - \frac{2C_{23}.\gamma_e}{r_0.R.\mathrm{tg}\,\delta} + \frac{2C_{33}.T.\sin\delta(e_0 + R\sin\delta)}{r_0.(R - R')} \tag{23}$$

$$\varepsilon_0 = e_0 - r_0(2.\sin\delta - \mathrm{tg}\,\delta) \quad \chi = \frac{e_0.\cos\delta}{(e_0\cos\delta - r_0\sin\delta)} \tag{24}$$

With Equation (16), one can analyze the relationship between the critical speed and the mechanical characteristic parameters. λ_i is the corresponding value of the matrix D, for any λ_i, assuming that its real part is $Re(\lambda_i)$. If $Re(\lambda_i)\rangle 0$ the corresponding motion mode is unstable.

Figures 10 and 11 show the relationship between the critical speed and the rail inclination considering the value of wheel equivalent conicity ($\gamma_e = 0.03$, 0.06, 0.12, 0.2 and 0.3) and the load per wheelset ($W = 17\,000$ kg, $W = 0$ kg). In addition, one can see the existence of a steep "cliff" at which the critical speed changes dramatically and the wheelset becomes unstable with small change on the angle of rail inclination. The values of equivalent conicity and the corresponding critical speed are listed in Table 1.

From the result shown in Table 1, one can deduce that the angle of rail inclination β is the same for charged or free wheelset and imposes a different critical speed. To examine the numerical result and analyze the relationship between critical speed and mechanical characteristic, one can see that a variation in the geometry (angle rail inclination) has much greater influence on the motion curve

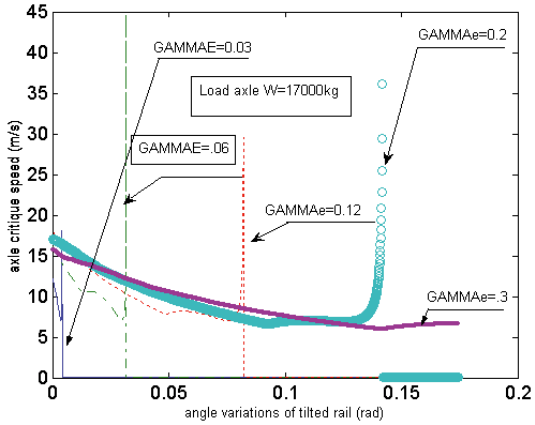

Fig. 11. Wheelset critical speed as function of rail inclination angle ($W = 17\,000$ kg).

Table 1. Critical speed of wheelset function of equivalent conicity.

V_c (m.s^{-1})	V_c (m.s^{-1})	Equivalent conicity (γ_e)	β (rd)
7.5	3	0.03	0.005
7.5	3	0.06	0.032
9	4	0.12	0.084
12.5	4	0.2	0.144
15	4	0.3	0.259
W= 17 000 kg	W = 0 kg		

(Figs. 5 and 6), but the corresponding critical speed is not much different from those obtained using classical rail.

For various values of the angle β and equivalent conicity, one notices that the critical speed of a free wheelset is 4 m.s^{-1} and that of a loaded wheelset is 15 m.s^{-1}. These critical speeds of wheelset are not different from those of wheelset circulating on classical rails. According to the results obtained in simulation, one can say that the rail inclinations preserve the same transverse stability in a classical vehicle.

4 Conclusion

A rail inclination is considered to improve the ability of the vehicle to steer around curves and to preserve a good stability. The writing of the dynamic equations of a vehicle moving on rail inclinations needs geometrical characteristics of these contact points between the wheel and the rail. A theoretical study is presented in Appendix A to determine these geometrical has characteristics. The simulation of the dynamic study of a vehicle moving on rail inclination is made on Matlab software. The effects of the longitudinal rigidity of primary suspension, radius curve, a angle of inclination of the rails and wheel equivalent conicity are considered to evaluate the curving performance and the transverse stability. The results of simulation show that it is necessary to choose the value of longitudinal rigidity K_x of the primary suspension, the angle of inclination of the rails and equivalent conicity of the wheel to improve the ability to steer around a curve without a high transverse displacement and without contact flange. Under these conditions, the wear of both rail and wheel is attenuated, and the lifespan of the wheel and the rail is prolonged. The study of the stability of a charged wheelset moving on an rail inclined is comparable to the wheelset moving on a classical rail. One can note that the rail inclination does not improve stability but keeps the same behavior as a traditional rail. The performance of the vehicle to steer around a curve is better achieved through the use of the inclined rail. Indeed, the simulation results illustrate:

- a strong value of the equivalent conicity decreases the transverse displacement. Then, one can use a worn wheel profile in traffic in a curve; but one must check that the value of the equivalent conicity preserves a good stability of the vehicle;
- a low value of the longitudinal rigidity of primary suspension, but one must also check that the value of the primary suspension stiffness preserves a good stability of the vehicle;
- large radii curves and high angle of rail inclination;
- the transverse displacement of wheelsets is clearly inferior to the one obtained with classic rails;
- the critical speed of wheelset is almost the same as the one obtained with classical rails;
- the rail inclination has compatibility between high-speed stability and the behaviour in curves.

The study of vehicle's simulation has shown the important improvement of the vehicle's performance in circulation in a curve achieved via the use of inclined rails. The bigger the inclination is, the better the vehicle's behaviour becomes in circulation in a curve, then, it's possible to increase the vehicles speeds in curve. The rail inclinations do not improve the vehicle's stability. The results found in this article by simulation confirms that the adopted mathematical models are near to reality. Indeed the results of simulation are confirmed by the experiment.

Appendix A: Geometric study of contact rail-wheel

A.1 Formulation of the mathematical model

The geometrical contact study allows us to determine the main geometric elements, which are functions of geometry of rail and wheel for a vehicle moving on inclined rails. Thus, it must provide us with formulas to evaluate the distances between the centre of inertia and the points of contact as function of the position parameters of the wheelset. If one considers the real form of the rail and the wheel, the motion of the wheelset on the rail has a corresponding double contact point. On the one hand, a point of contact is on the rail, and on the other hand, another point is on the wheel.

A.1.1 Influence of the transverse displacement "y"

The displacement of each contact point at any position and the variations of the angle of the tangent common plans to the contact point are determined as functions of a wheelset transverse displacement y and yaw angle α of the wheelset. The problem includes eight unknowns which are δ'_1, δ'_2, r_1, r_2, e_1, e_2, ψ and z.

For the simplicity of calculation, one keeps the notation δ_0, δ_1 and δ_2. The final expressions will be expressed according to δ'_0, δ'_1 and δ'_2 (see Fig. 2).

A.1.1.1 Left wheel study ($j = 1$)

One sets A_1 and B_1, the common points of the wheel and rail for a central position of the wheelset and I_1 the contact point rail-wheel at any position of the wheelset (see Fig. 2). One can write:

$$\boldsymbol{G}_e\boldsymbol{A}_1 = \boldsymbol{G}_e\boldsymbol{G} + \boldsymbol{G}\boldsymbol{A}_1 \tag{A.1}$$

$$\boldsymbol{G}_e\boldsymbol{A}_1 = \boldsymbol{y}.\boldsymbol{y}_0 + z.\boldsymbol{z}_0 + e_0\boldsymbol{u}(\psi) - r_0\boldsymbol{u}\left(\psi + \frac{\pi}{2}\right) \tag{A.2}$$

and:

$$\boldsymbol{G}_e\boldsymbol{B}_1 = e_0\boldsymbol{y}_0 - r_0\boldsymbol{z}_0 \tag{A.3}$$

$$\boldsymbol{G}_e\boldsymbol{I}_1 = \boldsymbol{y}_0.(y + e_1\cos\psi + r_1\sin\psi) + \boldsymbol{z}_0(z + e_1\sin\psi - r_1\cos\psi) \tag{A.4}$$

Then, one deduces the following relations:

$$\boldsymbol{A}_1\boldsymbol{B}_1 = \boldsymbol{y}_0.(e_0 - y - e_0\cos\psi - r_0\sin\psi) + \boldsymbol{z}_0.(-r_0 - z - e_0\sin\psi + r_0\cos\psi) \tag{A.5}$$

$$\boldsymbol{B}_1\boldsymbol{I}_1 = \boldsymbol{y}_0.(y + e_1\cos\psi + r_1\sin\psi - e_0) + \boldsymbol{z}_0.(r_0 + z + e_1\sin\psi - r_1\cos\psi) \tag{A.6}$$

$$\boldsymbol{A}_1\boldsymbol{I}_1 = \boldsymbol{y}_0.[\cos\psi(e_1 - e_0) + \sin\psi(r_1 - r_0)] + \boldsymbol{z}_0.[\sin\psi(e_1 - e_0) - \cos\psi(r_1 - r_0)] \tag{A.7}$$

$$\boldsymbol{B}_1\boldsymbol{I}_1 = R'[(\cos\delta_1 - \cos\delta_0).\boldsymbol{z}_0 - (\sin\delta_1 - \sin\delta_0).\boldsymbol{y}_0] \tag{A.8}$$

Note:

The contact point I_1 imposes that $\boldsymbol{O}'_1\boldsymbol{I}_1$ and $\boldsymbol{z}_0$ make an angle δ_1. From Figure 12, one deduces the relations:

$$\boldsymbol{A}_1\boldsymbol{I}_1 = R.\big((\cos\delta_1 - \cos(\delta_0 + \psi)).\boldsymbol{z}_0 - (\sin\delta_1 - \sin(\delta_0 + \psi)).\boldsymbol{y}_0\big) \tag{A.9}$$

$$\boldsymbol{A}_1\boldsymbol{B}_1 = \boldsymbol{z}_0.((R - R')\cos\delta_1 - R\cos(\delta_0 + \psi) + R'\cos\delta_0) + \boldsymbol{y}_0(R\sin(\delta_0 + \psi) - R'\sin\delta_0 - (R - R')\sin\delta_1). \tag{A.10}$$

(6) and (10) give us the following relations:

$$e_0(1 - \cos\psi) - y - r_0\sin\psi = R\sin(\psi + \delta_0) - R'\sin\delta_0 - (R - R')\sin\delta_1. \tag{A.11}$$

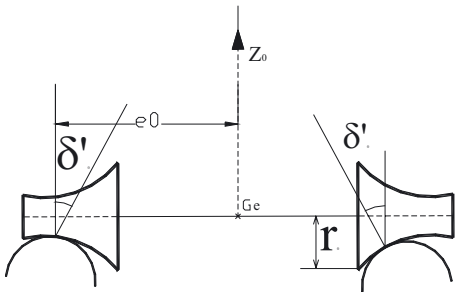

Fig. 12. Contact points of the wheelset for a central position.

$$r_0(\cos\psi - 1) - z - e_0\sin\psi = (R - R')\cos\delta_1 - R\cos(\psi + \delta_0) + R'\cos\delta_0. \tag{A.12}$$

From (A.7) and (A.9), we obtain:

$$y + e_1\cos\psi + r_1\sin\psi - e_0 = R'(\sin\delta_0 - \sin\delta_1) \tag{A.13}$$

$$z + e_1\sin\psi - r_1\cos\psi + r_0 = R'(\cos\delta_1 - \cos\delta_0) \tag{A.14}$$

(A.8) and (A.9) give us the following relations:

$$\cos\psi.(e_1 - e_0) + \sin\psi.(r_1 - r_0) = R.[-\sin\delta_1 + \sin(\psi + \delta_0)] \tag{A.15}$$

$$\sin\psi.(e_1 - e_0) - \cos\psi.(r_1 - r_0) = R.[\cos\delta_1 - \cos(\psi + \delta_0)] \tag{A.16}$$

Hence, one disposes of 6 non-linear Equations (A.11)–(A.16), in order to express the 8 unknowns δ_1, δ_2, r_1, r_2, e_1, e_2 , ψ and z in term of the transverse displacement y of the wheelset. It is assumed that the roll angle ψ is small. These equations become:

$$y + r_0.\psi = (R - R').(\sin\delta_1 - \sin\delta_0) - R.\psi.\cos\delta_0 \tag{A.17}$$

$$z + e_0.\psi = (R - R').(\cos\delta_0 - \cos\delta_1) - R.\psi.\sin\delta_0 \tag{A.18}$$

$$y + (e_1 - e_0) + r_1.\psi = R'.(\sin\delta_0 - \sin\delta_1) \tag{A.19}$$

$$z + e_1.\psi + r_0 - r_1 = R'.(\cos\delta_1 - \cos\delta_0) \tag{A.20}$$

A.1.1.2 Right wheel contact study ($j = 2$)

Obvious symmetry allows us to deduce the equations required for the right wheel, one replaces in the previous equations:

e_0 replaced by $-e_0$;
$e_1$replaced by $-e_2$;
r_1 replaced by r_2;
δ_0 replaced by $-\delta_0$;
δ_1 replaced by δ_2.

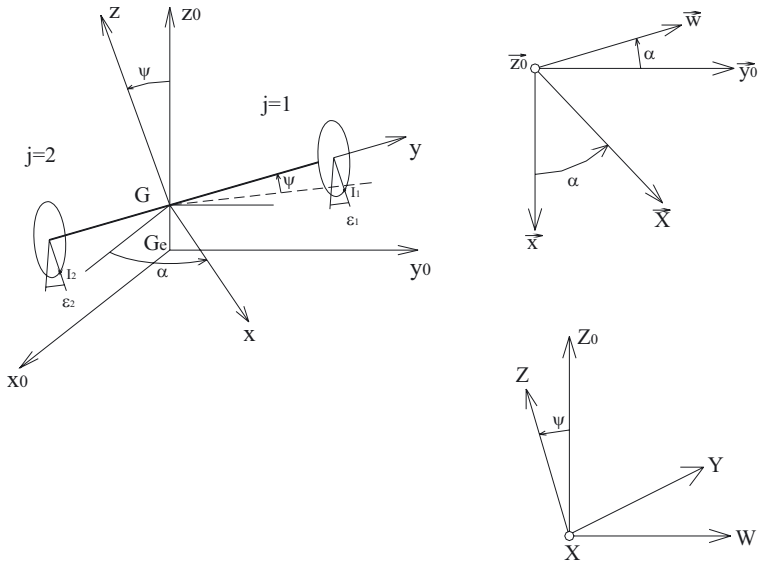

Fig. 13. Influence of yaw wheelset: contact points in space.

One obtains respectively the following relations:

$$y + r_0.\psi = (R - R').(\sin\delta_2 + \sin\delta_0) - R.\psi.\cos\delta_0 \tag{A.21}$$

$$z - e_0.\psi = (R - R').(\cos\delta_0 - \cos\delta_2) + R.\psi.\sin\delta_0 \tag{A.22}$$

$$y - (e_2 - e_0) + r_2.\psi = R'.(-\sin\delta_0 - \sin\delta_2) \tag{A.23}$$

$$z - e_2.\psi + r_0 - r_2 = R'.(\cos\delta_2 - \cos\delta_0) \tag{A.24}$$

A.1.1.3 Resolution of the system

Taking into account all the calculations, one finds the following expressions as functions of the transverse displacement y.

$$\psi = \frac{y\sin\delta_0'}{e_0\cos\delta_0' - r_0\sin\delta_0'} = \Gamma.y \qquad \text{with}$$

$$\Gamma = \frac{\sin\delta_0'}{e_0\cos\delta_0' - r_0\sin\delta_0'} \tag{A.25}$$

$$z = \frac{y^2}{2(R-R')\cos\delta_0'}\left(\frac{e_0 + R\sin\delta_0'}{e_0\cos\delta_0' - r_0\sin\delta_0'}\right)^2 \tag{A.26}$$

$$e_1 = e_0 - \gamma_e.y.\mathrm{cotg}\,\delta_0' \tag{A.27}$$

$$r_1 = r_0 + \gamma_e.y \tag{A.28}$$

$$e_2 = e_0 + \gamma_e.y.\mathrm{cotg}\,\delta_0' \tag{A.29}$$

$$r_2 = r_0 - \gamma_e.y \tag{A.30}$$

The results obtained are summarized above where "γ_e" is the equivalent conicity

$$\gamma_e = \frac{R\sin\delta_0'}{R - R'}\left(\frac{e_0 + R'\sin\delta_0'}{e_0\cos\delta_0' - r_0\sin\delta_0'}\right) \tag{A.31}$$

A.2.1 Rotation effect

The influence of the rotation α of the wheelset leads to the resolution of a space geometry. This rotation produces a three-dimensional displacement of the contact points and these points do not remain in the vertical plan containing the axis of the wheelset. It results in an increased number of unknowns. G_e coincides with G for a central position. The contact points on the left wheel are indicated by I_1 and those on the right wheel by I_2. X_i, Y_i, Z_i are the Cartesian coordinates of I_i $(i = 1, 2)$. The cylindrical coordinates r_i, ε_i and e_i of these contact points allow us to define their position on the wheelset. The number of unknowns is now 16:

- Cartesian coordinates of contact points: X_i, Y_i, Z_i.
- polar coordinates of contacts points: r_i, e_i, ε_i
- rotation of the wheelset: ψ (about axis x).
- level variation height of inertia centre z.
- angle between the contact plan and horizontal δ_i.

The Cartesian coordinates of the points of contact are only introduced to give more clearity to the mathematical reasoning.

The used method consists in writing that each contact point belongs to the rail and the wheel by imposing the direction of the normal vectors to both profiles at the contact points at which they coincide. Calculations will preserve terms of the second order and linearization is used only if that is necessary for the resolution of the system. The contact of the left and the right wheel is examined separately.

A.2.2.1 Left wheel contact study ($j = 1$)

For a central position of the wheelset, the contact in B_1 makes an angle δ_0' with the vertical. Let (Δ) be the longitudinal axis of cylinder rail scheme, and O_1' the point

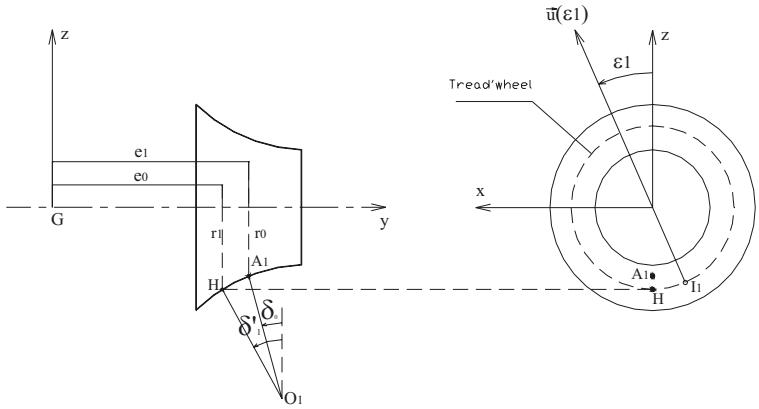

Fig. 14. Wheel contact points in space.

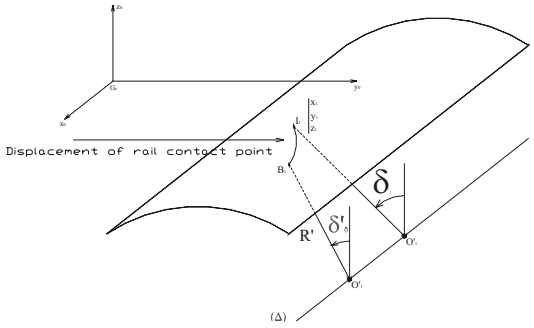

Fig. 15. Influence of yaw wheelset: contact points in space.

of this axis located in the plan (G_e, Y_0, Z_0) (Fig. 16). Then, one can write:

$$\boldsymbol{O'_1G}_e = \boldsymbol{O'_1B}_1 + \boldsymbol{B}_1\boldsymbol{P} + \boldsymbol{PG}_e$$
$$= R'.\boldsymbol{u}\left(\delta_0 + \frac{\pi}{2}\right) + r_0.\boldsymbol{z}_0 - e_0.\boldsymbol{y}_0 \quad \text{(A.32)}$$

$$\boldsymbol{O'_1G}_e = (R'\cos\delta_0 + r_0).\boldsymbol{z}_0 - (e_0 + R'\sin\delta_0).\boldsymbol{y}_0 \quad \text{(A.33)}$$

For a rotation α of the wheelset, the contact point B_1 moves on the rail until I_1, while O'_1 comes in O''_1. The line (O''_1I_1) makes an angle δ_1 with the vertical. A_1 is the point of wheel in contact with the rail for a central position, and H the point situated on the rolling circle contained in the plan (G, Y, Z), (see Fig. 15). $\boldsymbol{N}_1$ is the normal to the wheel surface to the point I_1. This vector is contained in the plan $(G\boldsymbol{Y}, \boldsymbol{u}(\boldsymbol{\varepsilon}_1))$ and makes an angle δ'_1 with $\boldsymbol{u}(\boldsymbol{\varepsilon}_1)$ (see Fig. 16). For the left wheel the following system is obtained:

$$R'(\sin\delta_0 - \sin\delta_1) =$$
$$e_1.\left(1 - \frac{\psi^2}{2} - \frac{\alpha^2}{2}\right) + r_1.\psi - r_1.\varepsilon_1.\alpha - e_0 \quad \text{(A.34)}$$

$$R'(\cos\delta_1 - \cos\delta_0) =$$
$$z + e_1.\psi - r_1.\left(1 - \frac{\psi^2}{2} - \frac{\varepsilon_1^2}{2}\right) + r_0 \quad \text{(A.35)}$$

$$R(\psi.\sin\delta_1.\left(1 - \frac{\alpha^2}{2} + \frac{\varepsilon_1^2}{2}\right) +$$
$$\cos\delta_1\left(1 - \frac{\psi^2}{2} + \frac{\varepsilon_1^2}{2}\right) - \cos\delta_0) = r_0 - r_1 \quad \text{(A.36)}$$

$$R(\sin\delta_0 - \sin\delta_1\left(1 - \frac{\psi^2}{2} - \frac{\alpha^2}{2}\right) + \psi.\cos\delta_0\right) = e_1 - e_0 \quad \text{(A.37)}$$

A.2.2.2 Right wheel contact study ($j = 2$)

Apparent symmetries allow us to deduce the system of equations for the right wheel. The following replacements in the previous Equations (A.34)–(A.37) are introduced:

e_0 replaced by $-e_0$
$e_1$replaced by $-e_2$
r_1 replaced by r_2
δ_0 replaced by $-\delta_0$
δ_1 replaced by δ_2
ε_1 replaced by ε_2.

The following equations are found:

$$R'(\sin\delta_0 + \sin\delta_2) =$$
$$-e_2.\left(1 - \frac{\psi^2}{2} - \frac{\alpha^2}{2}\right) + r_2.\psi - r_2.\varepsilon_2.\alpha + e_0 \quad \text{(A.38)}$$

$$R'(\cos\delta_2 - \cos\delta_0) =$$
$$z - e_2.\psi - r_2.\left(1 - \frac{\psi^2}{2} - \frac{\varepsilon_2^2}{2}\right) + r_0 \quad \text{(A.39)}$$

$$R(\psi.\sin\delta_2.\left(1 - \frac{\alpha^2}{2} + \frac{\varepsilon_1^2}{2}\right) + \cos\delta_2\left(1 - \frac{\psi^2}{2} + \frac{\varepsilon_1^2}{2}\right)$$
$$-\cos\delta_0) = r_0 - r_2 \quad \text{(A.40)}$$

$$R(\sin\delta_0 + \sin\delta_2\left(1 - \frac{\psi^2}{2} - \frac{\alpha^2}{2}\right) - \psi.\cos\delta_2) = e_2 - e_0 \quad \text{(A.41)}$$

A.2.2.3 Resolution of system

The following solutions are obtained with the second order:

$$\psi = 0 \tag{A.42}$$

$$z = \frac{\alpha^2 \mathrm{tg}\,\delta_0'}{2} \cdot [r_0(2\sin\delta_0' + \mathrm{tg}\,\delta_0') - e_0] \tag{A.43}$$

$$\varepsilon_1 = -\alpha \cdot \mathrm{tg}\,\delta_0' \tag{A.44}$$

$$r_1 = r_0 + R.\mathrm{tg}\,\delta_0' \cdot \left(\frac{(R+2r_0)\sin\delta_0' - e_0}{R-R'} - \sin\delta_0'\right) \cdot \frac{\alpha^2}{2} \tag{A.45}$$

$$e_1 = e_0 + \frac{R}{R-R'}\left(e_0 - (R'+2r_0)\sin\delta_0'\right)\frac{\alpha^2}{2} \tag{A.46}$$

$$\varepsilon_2 = \alpha \cdot \mathrm{tg}\,\delta_0' \tag{A.47}$$

$$r_2 = r_0 + R.\mathrm{tg}\,\delta_0' \cdot \left(\frac{(R+2r_0)\sin\delta_0' - e_0}{R-R'} - \sin\delta_0'\right) \cdot \frac{\alpha^2}{2} \tag{A.48}$$

$$e_2 = e_0 + \frac{R}{R-R'}\left[e_0 - (R'+2r_0)\sin\delta_0'\right]\frac{\alpha^2}{2} \tag{A.49}$$

$$\begin{aligned}
\sin\delta_1' &= \sin\delta_0' + \frac{y}{R-R'}\left(\frac{e_0\cos\delta_0' + R\cdot\sin\delta_0'\cdot\cos\delta_0'}{e_0\cos\delta_0' - r_0.\sin\delta_0'}\right)\\
\sin\delta_2' &= -\sin\delta_0' + \frac{y}{R-R'}\left(\frac{e_0\cos\delta_0' + R\cdot\sin\delta_0'\cdot\cos\delta_0'}{e_0\cos\delta_0' - r_0\cdot\sin\delta_0'}\right)\\
\cos\delta_1' &= \cos\delta_0' - \frac{z}{R-R'} - \frac{\psi}{R-R'}(e_0 + R\sin\delta_0')\\
\cos\delta_2' &= \cos\delta_0' - \frac{z}{R-R'} + \frac{\psi}{R-R'}(e_0 + R\sin\delta_0')
\end{aligned} \tag{A.50}$$

The final expressions of these geometrical quantities take into account the influence of the transverse displacement "y" and rotation "α", these quantities are obtained by adding the previously established results. In the majority of the expressions above, rotation. "α" intervenes only with the second order.

A.3. Conclusion

The geometric study results are used to write the expressions of the kinetic energy, the force function, and the dissipated power to determine the motion equations of the vehicle. This geometrical study shows the fundamental importance of the profile of the rail and the wheel. From the dynamical model, one can study the influence of the geometry of both wheel and rail on the behaviour of the vehicle. The best results of the behaviour of the vehicle in alignment and curve indicate the geometric characteristics to be given to the wheel and the rail. Indeed, these profiles change in the course of time that means that the expressions of e_1, r_1, e_2, r_2 are functions of time.

References

[1] H. Bettaieb, Étude de la stabilité transversale et le comportement en courbe d'un véhicule ferroviaire, Doctorat 3e cycle mécanique appliqué à la construction, Université de Paris 6, 1983

[2] H. Bettaieb, R. Joly, Modélisation d'un véhicule ferroviaire en circulation en courbe, Les annales maghrébines de l'ingénieur 7 (1993) 107–120

[3] D. Boocok, Steady state motion of railway vehicle on curved track, J. Mech. Eng. 11 (1969) 556–566

[4] V. Rao, A.S. Dukkipati, S. Narrayana, Lateral stability and steady state curving performance of unconventional rail trucks, Mechanism and machine theory 136 (2001) 577–587

[5] P. Arus, A.D. de Pater, P. Meyers, The stationary Motion of a one-wheelset vehicle along a circular curve with real rail and wheels profiles, Vehicle system dynamics 37 (2002) 29–58

[6] F.F. Cheli, G. Diana, F. Resta, Numerical model of titling body railway vehicle compared with rig and on track tests, Vehicle system dynamics 35 (2001) 417–442

[7] Y. Sato, Design of rail head profiles with full use of grinding, Wear 144 (1991) 363–372

[8] J.F. Leary, S.N. Hand, B. Rajkumar, Development of freight car wheel profiles, Wear 144 (1991) 353–362

[9] R.E. Smith, A design for wheel and rail profiles for use on steered railway vehicles, Wear 144 (1991) 329–342

[10] J.J. Kalker, On the rolling contact of two elastic bodies in the presence of dry friction, Ph.D. thesis, Delft university of technology, 1967

[11] R. Joly, Traffic of a rail transit car on short radius curves, J. Theor. Appl. Mech. 4 (1985) 813–832